# Species-specific polyamines from diatoms control silica morphology

**Nils Kröger, Rainer Deutzmann, Christian Bergsdorf, and Manfred Sumper***

Lehrstuhl Biochemie I, Universität Regensburg, 93053 Regensburg, Germany

Communicated by Meinhart H. Zenk, University of Munich, Munich, Germany, October 19, 2000 (received for review October 1, 2000)

**Biomineralizing organisms use organic molecules to generate species-specific mineral patterns. Here, we describe the chemical structure of long-chain polyamines (up to 20 repeated units), which represent the main organic constituent of diatom biosilica. These substances are the longest polyamine chains found in nature and induce rapid silica precipitation from a silicic acid solution. Each diatom is equipped with a species-specific set of polyamines and silica-precipitating proteins, which are termed silaffins. Different morphologies of precipitating silica can be generated by polyamines of different chain lengths as well as by a synergistic action of long-chain polyamines and silaffins.**

The biological formation of inorganic structures, termed biominerals, is a widespread phenomenon in nature (1). Among the most famous examples are unicellular algae—diatoms—that possess a cell wall composed of silica and organic molecules or macromolecules (2). Most interestingly, diatom biosilica displays a dazzling variety of species-specific silica patterns that are structured on a nanometer-to-micrometer scale (3–6). Elucidating the mechanism that controls production of nanostructured biosilica is a fascinating biochemical problem and, in addition, is of great interest in materials chemistry. Biomimetic approaches are believed to allow the production of advanced materials at ambient temperature and with high precision, which are expected to exhibit superior properties in a wide range of applications (7, 8). Reaching this goal, however, requires a detailed knowledge of the organic molecules that govern silica biomineralization.

Recently, cationic polypeptides (called silaffins) isolated from purified cell walls of the diatom *Cylindrotheca fusiformis* were shown to generate networks of silica nanospheres within seconds when added to a solution of silicic acid (9). The silaffins are tightly associated with the biosilica so that they can only be solubilized after dissolution of the cell wall in hydrogen fluoride (HF). Silaffin-1 contains a previously undescribed type of protein modification, a polyamine consisting of 6–11 repeats of the *N*-methyl-propylamine unit (a mass increment of 71 Da per repeat) covalently attached to specific lysine residues (9). It is probably this structural element that accelerates silicic acid polymerization and promotes production of nanosphere networks. Previously, ultrastructural work on cell wall biogenesis in a number of diatoms led to the conclusion that silica appears to be deposited in different forms during valve morphogenesis. Especially evident was the participation of silica spheres ranging up to 100 nm in diameter (4, 10). If silaffins are indeed involved in the process of pattern formation that creates the amazingly rich variety of diatom shell silica structures, then different diatom species are expected to contain different types of silaffins or silaffin-like molecules. We therefore analyzed the HF-extractable organic cell wall components from a wide range of diatom species. Surprisingly, the cell wall of each diatom contains not only a species-specific set of silica-precipitating proteins (silaffins) but also high amounts of long-chain polyamines. In the present study, we report the structure of these polyamines and show that they occur in species-specific variations. If added to monosilicic acid solutions, the polyamines induce rapid precipitation of silica and are capable of controlling silica sphere size *in vitro*. Our data suggest that the combined action of silaffins and polyamines may mediate the formation of the species-specific biosilica patterns found in nature.

## Materials and Methods

**Culture Conditions.** Axenic unialgal cultures of *C. fusiformis* and *Nitzschia angularis* were kindly provided by B. E. Volcani (Scripps Institute of Oceanography, University of California at San Diego, La Jolla). *Chaetoceros debilis*, *Chaetoceros didymum*, *Eucampia zodiacus*, and *Stephanopyxis turris* were isolated from the North Sea and cultivated as axenic unialgal cultures in an artificial seawater medium according to the recipe from the North East Pacific Culture Collection (www.ocgy.ubc.ca/projects/nepcc/media.htm).

**Purification of Polyamines.** The following purification protocol was optimized for purification of *C. didymum* polyamines and was applied with slight modifications for purification of polyamines from all of the other diatom species. Harvested cells were boiled twice in 2% SDS/100 mM EDTA to remove intracellular components and membranes. Cell walls were pelleted by centrifugation (2,800 × *g*), extracted with acetone, washed extensively with $H_2O$, dried, and dissolved in liquid HF. After 30 min at 0°C, HF was evaporated, and any remaining material was dissolved in water. This extract was neutralized and loaded onto a HighS cation exchange column (Bio-Rad). The column was washed with 50 mM ammonium acetate, and polyamines were eluted with 2 M NaCl/20 mM $NaCO_3$, pH 10.0. The eluate was size fractionated on a Superose 12 h 10/30 column (Amersham Pharmacia; running buffer 250 mM NaCl/20 mM Tris·HCl, pH 7.5; flow was 0.25 ml/min), and fractions were analyzed for polyamines by Tris-Tricine [*N*-tris(hydroxymethyl)glycine] SDS/PAGE (11) with subsequent Coomassie blue staining. Polyamine-containing fractions were pooled, concentrated by lyophylization, and loaded onto a Superdex-Peptide HR 10/30 column (Amersham Pharmacia; running conditions as above) that achieves high resolution in the low molecular mass range. Fractions were analyzed as above, and polyamine-containing fractions were dialyzed against 5 mM ammonium acetate (Spectra/Por CE dialysis tubing; molecular mass cutoff 500 Da). The dialyzed samples were dried by lyophylization, and the residue was dissolved in $H_2O$.

**Mass Spectrometry of Polyamines.** Electrospray ionization/MS and fragmentation analysis were performed by using an Ion Trap ESQUIRE LC instrument (Bruker, Billerica, MA). Samples were infused by a nanospray source in 1 mM ammonium acetate, 50% $CH_3CN$.

*To whom reprint requests should be addressed. E-mail: manfred.sumper@vkl.uni-regensburg.de.

The publication costs of this article were defrayed in part by page charge payment. This article must therefore be hereby marked "*advertisement*" in accordance with 18 U.S.C. §1734 solely to indicate this fact.

Article published online before print: *Proc. Natl. Acad. Sci. USA*, 10.1073/pnas.260496497. Article and publication date are at www.pnas.org/cgi/doi/10.1073/pnas.260496497

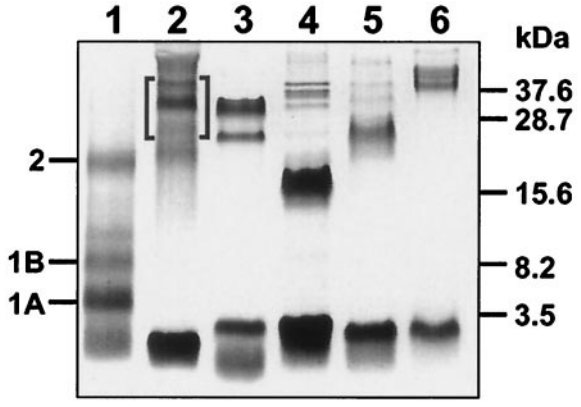


**Fig. 1.** HF extracts from diatom cell walls. Extracts were subjected to Tris-Tricine SDS/PAGE (11) and stained with Coomassie blue. Lanes: 1, *C. fusiformis* (positions of silaffin species are marked); 2, *N. angularis*; 3, *C. didymum*; 4, *C. debilis*; 5, *E. zodiacus*; 6, *S. turris*. The brackets in lane 2 mark the three silaffins that were used for silica precipitation (see Fig. 6).

**Quantification of Polyamines.** Polyamines were semiquantitatively detected by a modification of a described staining method that detects primary, secondary, and tertiary amines on TLC plates (12). Each 0.5 $\mu$l of different dilutions of the polyamine solution was dotted onto a nitrocellulose membrane. The dried membrane was laid on a filter paper soaked with an aqueous cobalt thiocyanate solution (2 M ammonium thiocyanate/200 mM cobalt chloride hexahydrate). Polyamine-containing spots appear light blue on a purple background. The synthetic polyamine DAB-Am-16 (Aldrich) served as a reference. This compound is a dendrimer with a molecular mass of 1,686.8 Da that is made up of aminopropyl units attached to a putrescine residue.

**Silica Precipitation and Field-Emission Scanning Electron Microscopy Analysis.** Silica precipitation and quantification was performed as described (9). For electron microscopy, washed silica precipitates were resuspended in $H_2O$, mounted on a coverslip, and air dried. The specimens were briefly sputter-coated with Pd/Au and analyzed on an LEO1530 field-emission scanning electron microscope.

**Enrichment of *N. angularis* Silaffins.** The first steps were performed as described for purification of polyamines. Fractions from the Superose 12 column (Amersham Pharmacia; running buffer 250 mM NaCl/20 mM Tris·HCl, pH 7.5; flow was 0.25 ml/min) eluting between 12.8–13.9 ml were pooled and dialyzed against 5 mM ammonium acetate (Spectra/Por CE dialysis tubing; molecular mass cutoff 1,000 Da). Protein concentration was determined by the bicinchoninic acid assay (13).

## Results

Diatom cell walls were isolated from six different species, *C. fusiformis*, *N. angularis, C. didymum*, *C. debilis*, *E. zodiacus*, and *S. turris* (see *Materials and Methods*), and were dissolved in anhydrous HF. The resulting soluble material was subjected to a special variant of PAGE (11) that is adapted to resolve low molecular weight components (Fig. 1). Compared with the silaffin pattern obtained from *C. fusiformis* (Fig. 1, lane 1), it is quite evident that each diatom species contains a species-specific set of polypeptides. As all these proteins have strongly basic properties (data not shown), they are likely to represent different silaffin species. Remarkably, an extremely low molecular mass material of less than 3.5 kDa is a main component in all of these newly analyzed diatoms. This material is not as evident in the originally investigated diatom *C. fusiformis*.

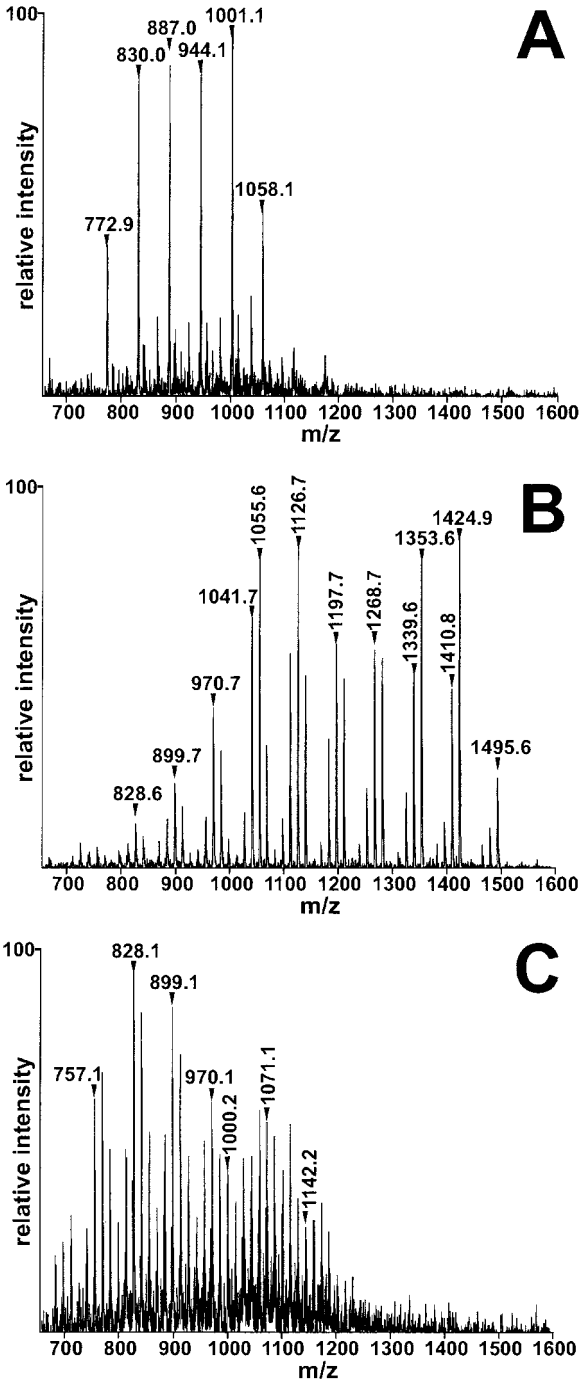


**Fig. 2.** Characterization of diatom polyamines. Electrospray ionization/MS analysis of purified polyamine fractions. Each peak represents a singly charged positive ion. Selected peaks are marked by their $m/z$ units. (*A*) *C. fusiformis* polyamines. (*B*) *C. didymum* polyamines. (*C*) *N. angularis* polyamines.

We purified these low molecular mass materials from *C. fusiformis*, *C. didymum*, and *N. angularis* by absorption to a cation exchange matrix from which elution could be achieved only under high-salt (2 M NaCl) conditions. This behavior suggests a polycationic structure for these substances. Final purification by size-exclusion chromatography yielded preparations that appeared homogenous in SDS gel electrophoresis (not shown). The mass spectra (electrospray ionization) of the purified materials are documented in Fig. 2. Surprisingly, each preparation does

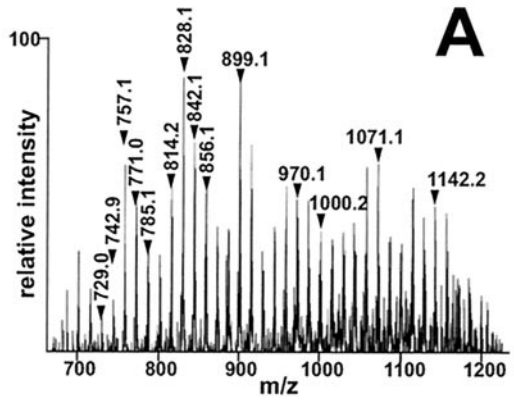


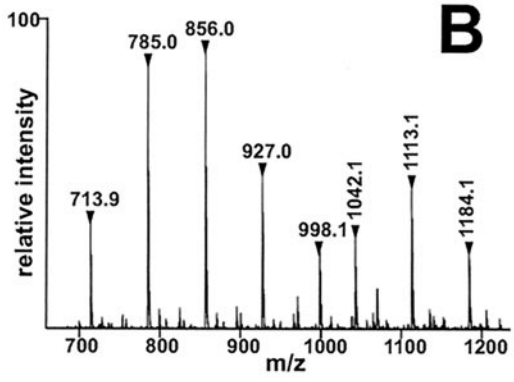


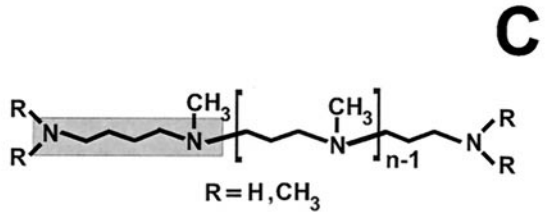


D

| chain length n | R = [4 × H, —] (Da) | [3 × H, 1 × $CH_3$] (Da) | [2 × H, 2 × $CH_3$] (Da) | [1 × H, 3 × $CH_3$] (Da) | [—, 4 × $CH_3$] (Da) |
|---|---|---|---|---|---|
| 8 | 657.8 | 671.7 | 685.7 | 699.8 | **713.8** |
| 9 | 728.8 | 742.8 | 756.8 | 770.8 | **784.8** |
| 10 | 799.9 | 813.9 | 827.9 | 841.9 | **855.9** |
| 11 | 871.0 | 885.0 | 899.0 | 913.0 | **927.0** |
| 12 | 942.1 | 956.0 | 970.0 | 984.1 | **998.1** |

**Fig. 3.** Permethylation analysis of the polyamines from *N. angularis*. (*A* and *B*) Electrospray ionization/MS analysis of singly charged positive ions. (*A*) Unmodified polyamines from *N. angularis*. Two peak series, which are separated by 71 units, are denoted by vertical numbers that indicate the *m*/*z* value of the corresponding peak. Within each series, peak masses differ by 14 units. The horizontal numbers indicate selected molecules whose masses differ by 71 units. (*B*) Polyamines from *N. angularis* after permethylation. Two peak series can be discerned, which are denoted by horizontal numbers (putrescine basis) and vertical numbers (ornithine basis), respectively. Within each series, peak masses differ by 71 units. (*C*) Scheme of proposed general polyamine structure. The gray box highlights the putrescine moiety. (*D*) Theoretical molecular masses of putrescine-based polyamine molecules. Each line corresponds to a given polyamine chain length and lists the theoretical molecular masses of methylation isoforms. The molecular masses of fully methylated isoforms are boxed.

not contain a single molecular species but rather consists of a complex population of molecules with masses ranging from ≈600–1,500 Da. Even more surprising is the fact that each of these diatom species contains a unique collection of these substances. After subjecting these substances to conditions of strong acid hydrolysis (6 M HCl, 17 h at 110°C), their molecular masses remained unaffected. This result excludes the presence of a peptide moiety in these substances, as was found for silaffins. The least complex pattern is observed for the material from *C. fusiformis*, which appears to contain only six molecular species whose masses differ by multiples of 57 Da (Fig. 2*A*). The *C. didymum* material reveals quadruplets of mass peaks that are spaced by 71 Da. Within each quadruplet, neighboring peak masses differ by 14 Da (Fig. 2*B*). An even higher degree of complexity is observed in the peak pattern of *N. angularis* (Fig. 2*C*), yet this pattern may also be interpreted as being composed of multiple sets of peaks spaced by 71 Da. Within each set, peak masses differ by 14 Da. Mass differences of 71 Da among the members of a given population again indicate the presence of the *N*-methyl-propylamine building block as found in silaffin-1 (9). Mass differences of 14 units may indicate different degrees of methylation at as yet unknown positions. A mass increment of 57 Da (71−14 Da) suggests the existence of a nonmethylated propylamine moiety serving as the repeated unit.

Despite the complexity of the mass spectra, nearly all of the individual mass signals can be assigned if the following assumptions are made. All these substances represent linear long-chain polyamines with different numbers of the repeated unit *N*-methyl-propylamine (or propylamine). The resulting polyamines are attached either to ornithine or its decarboxylation product, putrescine. The putrescine (ornithine) moiety as well as the terminal propylamine unit displays different degrees of *N*-methylation, allowing a maximum of four additional methyl groups per molecule (Fig. 3*C*). The corresponding assignment for the main mass signals observed for the *N. angularis* polyamines (Fig. 3*A*) is given in Fig. 3*D*. If this interpretation holds, reductive methylation with formaldehyde and sodium cyanoborohydride should greatly reduce the complexity of the polyamine population. This reaction methylates primary as well as secondary amines to yield exclusively tertiary amino groups (14). By conversion of all of the partially *N*-methylated polyamine species to the completely *N*-methylated derivatives (Fig. 3*B*), the complexity of the mass spectrum indeed collapses to the predicted series of mass signals (boxed values in Fig. 3*D*). These masses differ by 71 Da, which is because of the difference in chain length of the polyamine moiety. The masses correspond to a polyamine attached to trimethyl-putrescine with an additional methyl group at the terminal repeated unit, nitrogen (Fig. 3*C*). The minor series of peaks with masses 1,042, 1,113, and 1,184 in Fig. 3*B* can be explained by the assumption that an ornithine moiety, the biosynthetic precursor of putrescine, serves as the attachment site for the repeated units.

Independent proof of the proposed polyamine structure was obtained by tandem MS. For this experiment, the 856-Da molecular species (Fig. 3*B*) of the permethylated polyamine population from *N. angularis* was isolated by using the ion trap

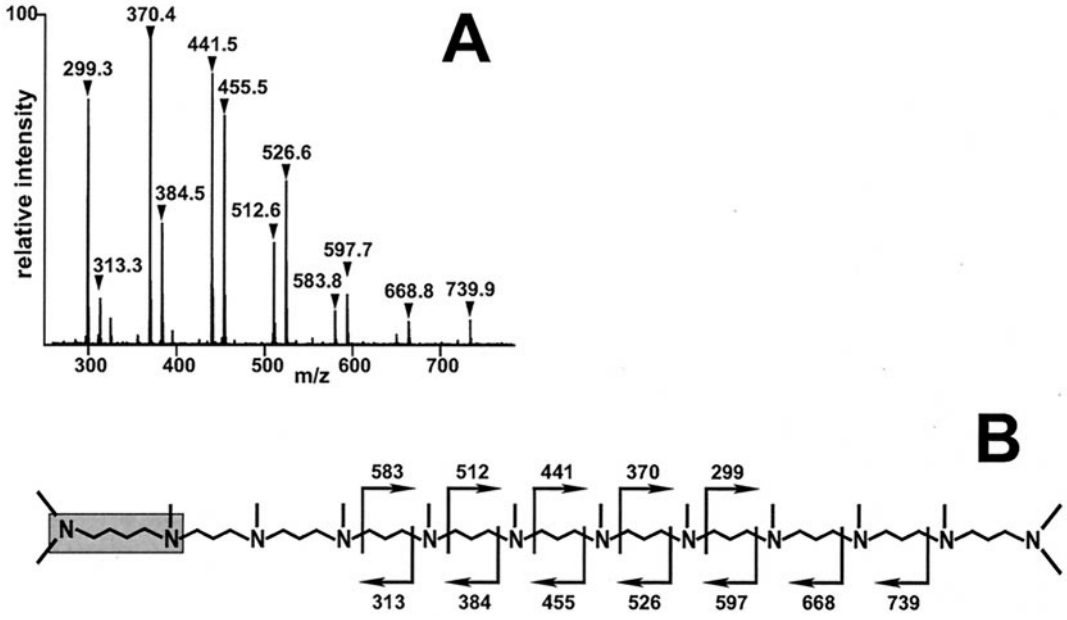


**Fig. 4.** Fragmentation analysis. (*A*) Product ion spectrum obtained by collision-induced fragmentation of the $(m + H)^+ = 856$ ion (see mass signal in Fig. 3*B*). Two series of ions were detected that differ by 14 units. Within each series, neighboring peaks differ by 71 units. (*B*) Proposed structure (schematic) of the $(m + H)^+ = 856$ ion. Cleavage positions that lead to the observed fragment ions are depicted by rectangular arrows, and the corresponding masses are indicated. The putrescine residue is highlighted by a gray box.

mode of the mass spectrometer followed by collision-induced fragmentation. The fragmentation pattern observed is documented in Fig. 4*A* and is in full agreement with the proposed structure of this molecule (Fig. 4*B*).

The same type of structural analysis was performed with the polyamines from the remaining two diatom species, and it fully confirmed the proposed structures. The polyamine population from *C. didymum* again consists of molecules with up to 20

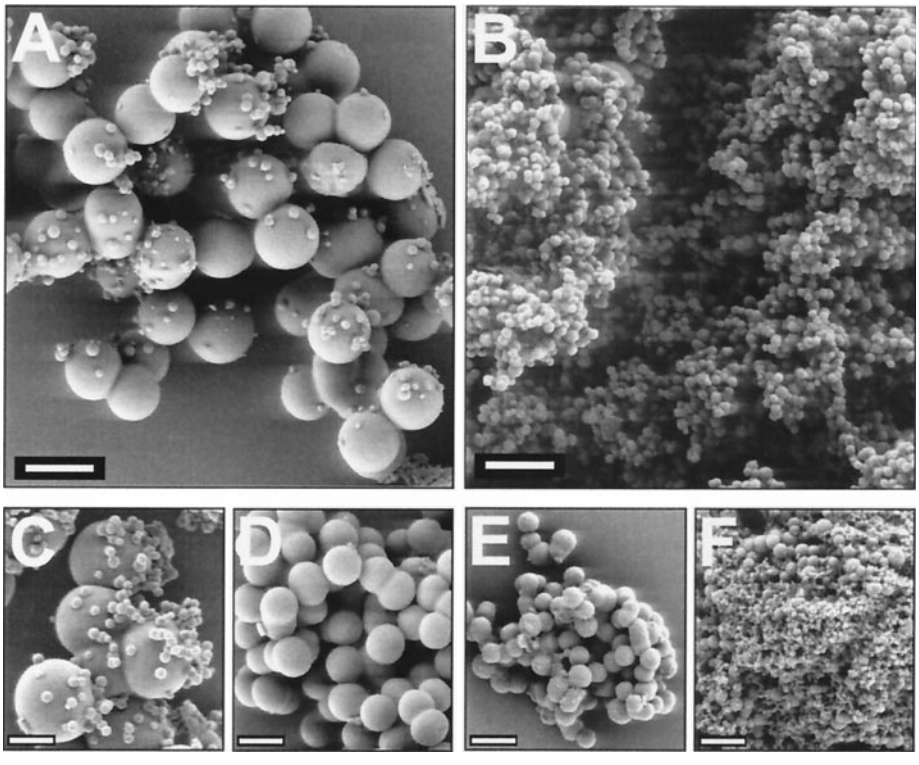


**Fig. 5.** Silica precipitates induced by *N. angularis* polyamines. For precipitation, polyamines of molecular masses from 1,000 to 1,250 (*A*) and 600 to 750 Da (*B*) were used. (*C–F*) The natural mixture of polyamines (molecular masses 600–1,250 Da) was used for investigating the pH dependence on polyamine-induced silica precipitation. (*C*) pH 5.4. (*D*) pH 6.3. (*E*) pH 7.2. (*F*) pH 8.3. The polyamine concentration in each solution was 0.85 mg/ml. [Scale bars, 1 $\mu$m (*A* and *B*) and 500 nm (*C–F*).]

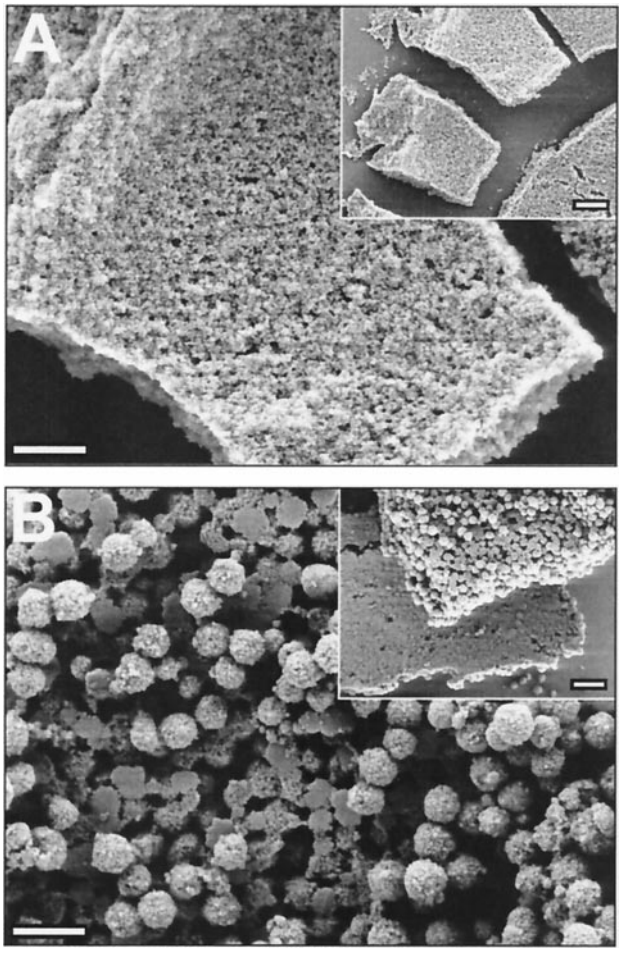


**Fig. 6.** Effect on silica morphology of combining *N. angularis* polyamines and silaffins. For precipitation in *A*, enriched silaffins (see brackets in Fig. 1, lane 2) at a concentration of 3 mg/ml were used and in *B*, a mixture of silaffins (3 mg/ml) and polyamines (0.85 mg/ml) was used. (*Insets*) Larger views of the precipitates. [Scale bars, 500 nm, 1 $\mu$m (*Insets*).]

repeated units of *N*-methyl-propylamine attached to methylation isoforms of putrescine. However, the construction mode of *C. fusiformis* polyamines differs from the general structure because it contains a 57-Da repeated unit (Fig. 2*A*). The molecular mass of the repeated unit of the *C. fusiformis* polyamines is altered on acetylation as well as methylation. Peracetylation by treatment with acetic anhydride increases the repeated unit size to 99 Da, whereas permethylation (14) results in a repeated unit size of 71 Da (data not shown). This indicates that in the *C. fusiformis* polyamines, each repeated unit element contains a single secondary amino group, which is converted by acetylation to an *N*-acetyl group (+42 Da per unit element) and by methylation to a tertiary *N*-methyl group (+14 Da per unit element). Together with data from the fragmentation analysis (not shown, these results are consistent with a putrescine-based polyamine structure with two terminal *N*-dimethyl groups and with secondary (nonmethylated) amino groups within the polyamine chain.

The presence of long-chain polyamines as major organic constituents of biosilica in all of the diatom species investigated strongly suggests that these molecules are general components of the silica biogenesis machinery. Indeed, when these polyamines are added to a silicic acid solution *in vitro* a precipitate forms after a few minutes that is composed of both silica and polyamines. The precipitate contains 1.25 $\mu$g of $SiO_2$ per 1 $\mu$g of polyamine. This stoichiometry suggests a tight interaction between the amino groups and the silanol groups of silica. Strong hydrogen-bonding interaction has been demonstrated for silica gel/amine hybrids that are composed of silica and synthetic polyallylamine (15). Polyamines are known to accelerate silicic acid polymerization (15) and, in addition, to favor precipitation of colloidal silica by serving as a flocculating agent (16). Thus, the positively charged polyamines interconnect negatively charged polysilicic acid particles by simultaneous electrostatic interactions on adjacent particles (17).

Therefore, we analyzed by field-emission scanning electron microscopy how different diatom polyamines affect the morphology of precipitating silica. The polyamine population from *N. angularis* was fractionated according to chain length by size-exclusion chromatography, and individual fractions were used for silica precipitation. When polyamines in the mass range of 1,000 to 1,250 Da were added to a silicic acid solution at pH 5.0, the precipitate formed was composed of aggregates of spherical silica particles (Fig. 5*A*). These aggregates are dominated by spheres of 800 nm–1 $\mu$m in diameter. At the surfaces of the large spheres, a small amount of smaller spheres are attached with diameters of only 100–200 nm. Remarkably, this picture is completely reversed by using a polyamine fraction of masses between 600 and 700 Da for silica precipitation. In this precipitate, the 100- to 200-nm spheres dominate, and the large spheres are almost absent (Fig. 5*B*). This effect is not caused by a difference in silica-precipitating activity because with each molecular mass fraction the same amount of silica was precipitated. At pH 5.0, no silica spheres with diameters in the intermediate range of 200 to 800 nm could be observed with any of the polyamine size fractions (data not shown). However, this situation is changed when silica precipitation is performed at higher pH values. When the natural mixture of *N. angularis* polyamines is used for precipitation, the diameter of silica spheres markedly decreases with the increasing pH of the silicic acid solution (Fig. 5 *C–F*).

Finally, we investigated the influence on silica morphology that is exerted in the presence of the silaffins from *N. angularis*. When a mixture of three silaffins from *N. angularis* (denoted by brackets in Fig. 1, lane 2) is added to a silicic acid solution at pH 5.0, large, porous silica blocks that are made up of dense aggregates of <50-nm-sized, irregularly shaped silica particles are precipitated almost instantly (Fig. 6*A*). This silica morphology is completely different from the spherical structures that are formed in the presence of polyamines (Fig. 5*C*). Remarkably, when a mixture of the three silaffins and the polyamines from *N. angularis* is used for precipitation, a hybrid silica structure is generated. This precipitate contains silica blocks that are composed of spherical silica particles and, thus, is reminiscent of both the precipitate that forms in the presence of silaffin only (see silica blocks in Fig. 6*A*) and the precipitate that forms in the presence of polyamines only (see 200-nm-sized silica spheres in Fig. 5 *A–C*). However, the large silica spheres (800 nm–1 $\mu$m in diameter) that are also characteristic of the polyamine-induced precipitate are completely missing. Instead, silica blocks with one rather flat side as well as flattened silica particles are present (Fig. 6*B*). These structural features demonstrate that polyamines and silaffins together exert a synergistic effect on the morphology of precipitating silica.

## Discussion

In the present study, long-chain polyamines of the oligo-*N*-methyl-propylamine type have been characterized as general components of diatom biosilica. In *C. fusiformis*, these polyamines are attached to the polypeptide backbone of silaffins (9), whereas in the other diatom species, they are linked to free amino acid derivatives. The surprising diversity of polyamines and silaffins in all of the diatoms investigated, together with the

silica precipitation activity of these compounds, suggests that they are involved in the species-specific patterning of diatom biosilica. Work in the diatom field demonstrated that silica appears to be deposited in different forms during valve biogenesis (18–21). These forms include spherical silica (19–21) as well as block-like structures (e.g., areolae walls in ref. 18). Remarkably, similar silica morphologies can be generated *in vitro* by adding silaffins or polyamines to a metastable silicic acid solution (Figs. 5 and 6*A*). Furthermore, the structural characteristics of the silica precipitates can be modulated by application of a mixture of silaffins and polyamines (Fig. 6*B*). A combinatorial action of stage specifically expressed subsets of silaffins and polyamines may offer a biochemical explanation for the biogenesis of specific silica morphologies during different stages of valve morphogenesis. Further studies of the properties of silaffins from different diatom species may prove or disprove this biochemical model of pattern formation.

Apart from their implications to the problem of diatom biosilica morphogenesis, polyamines may offer a new approach for silica nanotechnology. So far, the technical synthesis of silica spheres requires either strongly alkaline conditions (22) or high temperatures and long incubation times (17, 23). In contrast, chemically synthesized polyamines of the oligo-*N*-methylpropylamine type with a defined chain length could be used to produce monodisperse silica nanospheres at neutral or mildly acidic pH and ambient temperature. This may be a valuable tool in applications that need to preserve temperature-sensitive components or alkaline-labile functional groups attached to silica spheres.

At present, the mechanism of polyamine-induced acceleration of silicic acid polymerization and precipitation is not completely understood. Recently, it was shown by Mizutani *et al.* (15) that synthetic polyamine molecules like polyallylamine and poly-L-lysine are able to catalyze silicic acid polycondensation at pH 8.5. These authors suggested that the polyamine may act as an acid-base catalyst that facilitates the condensation reaction (siloxane-bond formation) between two monosilicic acid molecules. Accordingly, the transition state may be stabilized by two appropriately arranged amino groups within the polyamine backbone, one of which deprotonated (acting as the ''base'') and the other one protonated (acting as the ''acid''). By accepting a proton from a silicic acid molecule, the base would aid in the formation of the reactive silanolate group, whereas the acid would facilitate by protonation the release of a water molecule from the attacked silicic acid molecule. Although this mechanism provides a reasonable explanation for the polyamine-induced silica formation, it fails to explain why silica nanospheres of defined size classes are formed in the presence of diatom polyamines. Possibly, additional cooperative interactions between polyamine and polysilicic acid molecules lead to a supramolecular assembly that provides the template for the formation of silica nanospheres. To test this hypothesis further, studies with synthetic model polyamines of defined chain length and methylation patterns are required.

We thank G. Lehmann and E. Hochmuth for expert technical assistance. We are indebted to LEO Elektronenmikroskopie (Oberkochen, Germany) for help with field-emission scanning electron microscopy analysis. This work was supported by the Deutsche Forschungsgemeinschaft (SFB 521).

1. Lowenstam, H. A. (1981) *Science* **211,** 1126–1131.
2. Volcani, B. E. (1981) in *Silicon and Siliceous Structures in Biological Systems*, eds. Simpson, T. L. & Volcani, B. E. (Springer, New York), pp. 157–200.
3. Pickett-Heaps, J., Schmid, A. M. M. & Edgar, L. A. (1990) in *Progress in Phycological Research,* eds. Round, F. E. & Chapman, D. J. (Biopress, Bristol, U.K.), Vol. 7, pp. 1–169.
4. Gordon, R. & Drum, R. W. (1994) *Int. Rev. Cytol.* **150,** 243–372.
5. Mann, S. (1993) *Nature (London)* **365,** 499–505.
6. Oliver, S., Kupermann, A., Coombs, N., Lough, A. & Ozin G. A. (1995) *Nature (London)* **378,** 47–50.
7. Parkinson, J. & Gordon, R. (1999) *Trends Biotechnol.* **17,** 190–196.
8. Mann, S. & Ozin, G. (1996) *Nature (London)* **382,** 313–318.
9. Kröger, N., Deutzmann, R. & Sumper, M. (1999) *Science* **286,** 1129–1132.
10. Li, C. W. & Volcani, B. E. (1984) *Philos. Trans. R. Soc. London B* **304,** 519–528.
11. Schägger, H. & von Jagow, G. (1987) *Anal. Biochem.* **166,** 368–379.
12. Stahl, E. (1969) *Thin-Layer Chromatography* (Springer, Berlin).
13. Smith, P. K., Krohn, R. I., Hermannson, G. T., Malillia, A. K., Gartner, F. H., Provenzano, M. D., Fujimoto, E. K., Goeke, N. M., Olson, B. J. & Klenk, D. C. (1985) *Anal. Biochem.* **150,** 76–85.
14. Jentoft, N. & Dearborn, D. G. (1983) *Methods Enzymol.* **91,** 570–579.
15. Mizutani, T., Nagase, H., Fujiwara, N. & Ogoshi, H. (1998) *Bull. Chem. Soc. Jpn.* **71,** 2017–2022.
16. Lindquist, G. M. & Stratton, R. (1976) *J. Colloid Interface Sci.* **55,** 45–59.
17. Iler, R. K. (1979) *The Chemistry of Silica* (Wiley, New York).
18. Schmid, A. M. M. & Volcani, B. E. (1983) *J. Phycol.* **19,** 387–402.
19. Chiappino, M. L. & Volcani, B. E. (1977) *Protoplasma* **93,** 205–221.
20. Borowitzka, M. A. & Volcani, B. E. (1978) *J. Phycol.* **14,** 101–121.
21. Schmid, A. M. M. & Schulz, D. (1979) *Protoplasma* **100,** 267–288.
22. Stöber, W., Fink, A. & Bohn, E. (1968) *J. Colloid Interface Sci.* **26,** 62–69.
23. Brinker, C. J. & Scherer, G. W. (1990) *Sol-Gel Science* (Academic, Boston).